JACS
JOURNAL OF THE AMERICAN CHEMICAL SOCIETY

Article

pubs.acs.org/JACS

Modular Pathway Engineering of Diterpenoid Synthases and the Mevalonic Acid Pathway for Miltiradiene Production

Yongjin J. Zhou,[†,#,▽] Wei Gao,[§,∥,▽] Qixian Rong,[§] Guojie Jin,[†,#] Huiying Chu,[‡] Wujun Liu,[†] Wei Yang,[†] Zhiwei Zhu,[†,#] Guohui Li,[‡] Guofeng Zhu,[⊥] Luqi Huang,*[,§] and Zongbao K. Zhao*[,†]

[†]Division of Biotechnology, and [‡]State Key Laboratory of Molecular Reaction Dynamics, Dalian Institute of Chemical Physics, CAS, Dalian 116023, People's Republic of China

[§]Institute of Chinese Materia Medica, CACMS, Beijing 100700, People's Republic of China

[∥]School of Traditional Chinese Medicine, Capital Medical University, Beijing 100069, People's Republic of China

[⊥]Institute of Pathogen Biology, CAMS, Beijing 100730, People's Republic of China

[#]Graduate University of Chinese Academy of Sciences, Beijing 100049, People's Republic of China

Supporting Information

ABSTRACT: Microbial production can be advantageous over the extraction of phytoterpenoids from natural plant sources, but it remains challenging to rationally and rapidly access efficient pathway variants. Previous engineering attempts mainly focused on the mevalonic acid (MVA) or methyl-D-erythritol phosphate (MEP) pathways responsible for the generation of precursors for terpenoids biosynthesis, and potential interactions between diterpenoids synthases were unexplored. Miltiradiene, the product of the stepwise conversion of (*E*,*E*,*E*)-geranylgeranyl diphosphate (GGPP) catalyzed by diterpene synthases SmCPS and SmKSL, has recently been identified as the precursor to tanshionones, a group of abietane-type norditerpenoids rich in the Chinese medicinal herb *Salvia miltiorrhiza*. Here, we present the modular pathway engineering (MOPE) strategy and its application for rapid assembling synthetic miltiradiene pathways in the yeast *Saccharomyces cerevisiae*. We predicted and analyzed the molecular interactions between SmCPS and SmKSL, and engineered their active sites into close proximity for enhanced metabolic flux channeling to miltiradiene biosynthesis by constructing protein fusions. We show that the fusion of SmCPS and SmKSL, as well as the fusion of BTS1 (GGPP synthase) and ERG20 (farnesyl diphosphate synthase), led to significantly improved miltiradiene production and reduced byproduct accumulation. The MOPE strategy facilitated a comprehensive evaluation of pathway variants involving multiple genes, and, as a result, our best pathway with the diploid strain YJ2X reached miltiradiene titer of 365 mg/L in a 15-L bioreactor culture. These results suggest that terpenoids synthases and the precursor supplying enzymes should be engineered systematically to enable an efficient microbial production of phytoterpenoids.

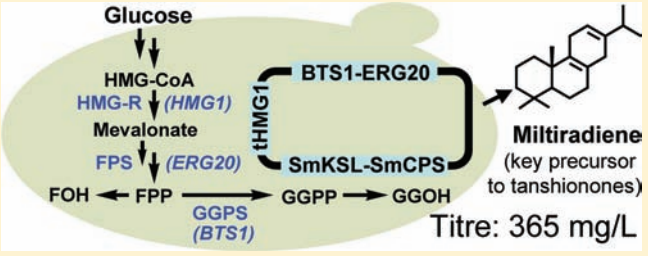

INTRODUCTION

Diterpenoids are 20-carbon terpenoids synthesized from (*E*,*E*,*E*)-geranylgeranyl diphosphate (GGPP) by diterpene synthases/cyclases. Some diterpenoids found in plants possess a wide range of pharmaceutical activities.[1] For example, the paclitaxel, a taxane diterpenoid from *Taxus brevifolia*, is a known antimicrotubule chemotherapy agent for the treatment of cancer.[2] Tanshionones are a group of abietane-type norditerpenoids rich in the Chinese medicinal herb *Salvia miltiorrhiza* (Supporting Information Figure 1), which have demonstrated a variety of biological activities, including antibacterial, antiinflammatory, and anticancer activities.[3] However, the extraction of diterpenoids from plants has been tedious and inefficient, and requires substantial sacrifice of natural resources.[4] Although a number of microorganisms have been engineered to produce isoprenoids as well as their intermediates,[5−7] the overall efficiency remains low. Further, there are complications that could have adverse effects on the engineered pathway. For example, metabolic flux imbalance, intermediates diffusion, and degradation can decrease the overall efficiency of the engineered pathway.[8] Thus, carefully tuning protein expression levels has been shown to balance the metabolic flux for improving productivity.[9] Artificial protein scaffolds capturing different stoichiometric number of enzymes in proximity have also been used in preventing intermediates loss.[10] These strategies commonly focus on the mevalonic acid (MVA) or methyl-D-erythritol phosphate (MEP) pathways that are at the early stage of terpenoids biosynthesis.[6,7,11] However, the conservation and interactions of diterpenoids synthases attracted little attention.

Received: December 7, 2011
Published: January 26, 2012

In nature, terpene synthases may contain one, two, or three highly conserved domains: the α domain with a highly α-helical fold containing a conserved DDXXD motif for Mg^{2+}-ionization and the $\beta\gamma$ domain often containing a catalytic DXDD motif for "protonization-initiated" catalysis.[12] The formation of the core structure of diterpenoids can be catalyzed by a bifunctional synthase or two consecutive enzymes (Figure 1a). The

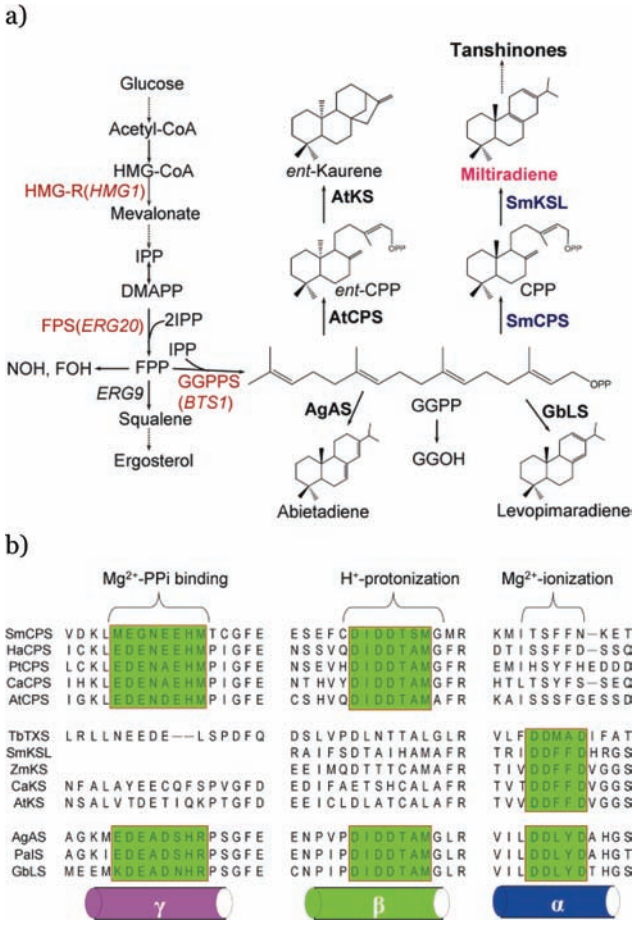

Figure 1. The diversity and conservedness of diterpenoids biosynthesis. (a) Schematic representation of the mevalonic acid (MVA) pathway and several diterpenoids biosynthetic pathways. Each solid arrow indicates a biosynthetic reaction step, and dashed arrows indicate the transformation involving multiple-step reactions. Abbreviations: HMG-CoA, 3-hydroxy-3-methylglutaryl coenzyme A; DMAPP, dimethylallyl diphosphate; IPP, isopentenyl pyrophosphate; GGOH, (*E*,*E*,*E*)-geranylgeraniol; CPP, copalyl diphosphate; *ent*-CPP, *ent*-copalyl diphosphate; HMG-R, HMG-coenzyme A reductase (encoded by the *HMG1* gene); FPPS, FPP synthase (*ERG20*); GGPPS, GGPP synthase (*BTS1*); SmCPS, copalyl diphosphate synthase of *S. miltiorrhiza*; SmKSL, kaurene synthase-like of *S. miltiorrhiza*; AtCPS, *ent*-copalyl diphosphate synthase of *Arabidopsis thaliana*; AtKS, kaurene synthase of *A. thaliana*; AgAS, abietadiene synthase of *Abies grandis*; GbLS, Levopimaradiene synthase of *Ginkgo biloba*. (b) ClustalW alignment of several diterpenoid synthases. Conserved catalytic motifs are highlighted, that is, DDxxD in α domain, DxDD in β domain, and D/E-rich region in γ domain involved in interactions with Mg^{2+} and GGPP.

bifunctional synthase such as AgAS contains functional $\alpha\beta\gamma$ domains (Figure 1b). In the case of two consecutive enzymes used, the first synthase is a class II cyclase containing domains $\alpha\beta\gamma$, but the α domain is a nonfunctional vestige due to the lack of the DDXXD motif. The second synthase is a class I enzyme containing either $\alpha\beta\gamma$ or $\alpha\beta$ domains, but only the α domain is functional, and the $\beta(\gamma)$ domain is vestigial due to the lack of the D/E-rich motif and the DXDD motif. No biochemical evidence has been known to support molecular interactions between the two consecutive enzymes, although such interactions are presumably beneficial for efficient substrate channeling in vivo to convert GGPP into diterpenoids.

We have recently demonstrated that in *S. miltiorrhiza* a labdadienyl/copalyl diphosphate synthase (SmCPS) and a kaurene synthase-like (SmKSL) are responsible for the transformation of GGPP into miltiradiene, the key intermediate to the pharmaceutically important compounds tanshinones (Figure 1a).[13] Here, we present the modular pathway engineering (MOPE) strategy and its application for a rapid assembling synthetic miltiradiene pathway in the yeast *Saccharomyces cerevisiae*. We analyzed the molecular interactions between SmCPS and SmKSL, and engineered their active sites into close proximity for enhanced metabolic flux channeling to miltiradiene biosynthesis by constructing protein fusions. We show that the fusion of SmCPS and SmKSL, as well as the fusion of BTS1 (GGPP synthase) and ERG20 (farnesyl diphosphate synthase), led to significantly improved miltiradiene production and reduced byproduct accumulation. Our most efficient pathway with the diploid strain YJ2X reached a miltiradiene titer of 365 mg/L in a 15 L bioreactor culture. These results suggested that engineering terpenoids synthases and the precursor supplying enzymes are essential for an efficient heterologous production of terpenoids in *S. cerevisiae*. Moreover, we showed that the fusion of enzymes catalyzing two consecutive reactions within the targeted pathway was in general helpful to improve the effectiveness of the engineered pathway.

RESULTS

The Interaction between Miltiradiene Synthases in Vivo. Sequence alignment suggested that SmCPS is a class II synthase containing $\alpha\beta\gamma$ domains, and SmKSL is a class I synthase containing the reserved Mg^{2+}-ionization motif DDXXD (Figure 1b). Because the cyclization of GGPP into diterpenoids can be realized by a number of bifunctional synthases, it is inspiring to speculate possible molecular interactions between the two miltiradiene synthases, SmCPS and SmKSL. To test our speculation, we performed coimmunoprecipitation experiments. The lysates of SmCPS-Flag and SmKSL-c-myc coexpressed cells were immunoprecipitated using anti-Flag M2 affinity gel, and then the lysates and eluates were analyzed by immunoblotting using anti-Flag and antimyc antibodies, respectively. Results showed SmKSL-c-myc was coprecipitated with SmCPS-Flag in anti-Flag eluates, indicating a direct interaction between SmCPS and SmKSL (Figure 2). This result suggested that SmCPS and SmKSL may form an enzyme complex in vivo. Although engineering the molecular interactions of diterpenoids synthases has not been demonstrated so far, these results encouraged us to fuse SmCPS and SmKSL for more efficient miltiradiene production (vide infra).

Optimization of the Mevalonate Pathway for Miltiradiene Production. We set up to engineer *S. cerevisiae* for miltiradiene overproduction. As our experiments suggested the presence of molecular interactions between SmCPS and SmKSL, we designed a series of pathway variants having these two proteins fused, hoping to improve productivity

dx.doi.org/10.1021/ja2114486 | J. Am. Chem. Soc. 2012, 134, 3234−3241

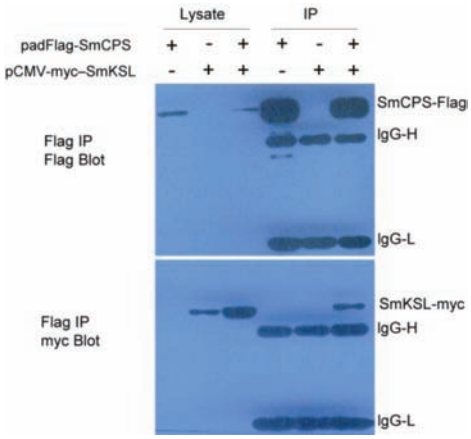

Figure 2. Sequential immunoprecipitation/immunoblot analysis of molecular interactions between SmCPS and SmKSL. The lysates of the transfected HEK-293T containing pad-Flag-SmCPS and/or pCMV-myc-SmKSL were immunoprecipitated using anti-Flag-agarose, and the precipitates were subjected to immunoblot analysis using Flag or c-Myc antibodies. The immune-blot revealed that SmKSL-myc was precipitated with SmCPS-Flag after anti-Flag-agarose immunoprecipitating.

(Figure 3a). Our first effort was the transformation of *S. cerevisiae* with the module producing SmCPS and SmKSL (YJ5), or the module producing the fused protein SmCPS-SmKSL (YJ1) or SmKSL-SmCPS (YJ2). However, miltiradiene production was undetectable for all of these three recombinant strains (Figure 3). One might think that SmCPS, SmKSL, and their fusions malfunctioned in yeast, but another possibility might be insufficient precursor supply. Therefore, we decided to make more pathway variants by using the MOPE strategy, which is an improved version of "DNA assembler".[14] In the MOPE strategy, each module was designed to have overlapping ends so that pathways can be generated rapidly in *S. cerevisiae* (Supporting Information Figure 2). We tried to enhance the MVA pathway in the YJ5 background. The modules *ERG20* and *BTS1* were quickly amended, either separately or fused by using the MOPE strategy. When the farnesyl diphosphate (FPP) synthase module *ERG20* was added, the resulting strain YJ6 produced a trace amount of miltiradiene. However, the strain YJ7 expressing the *BTS1* module produced 0.5 mg/L miltiradiene under shake flask culture conditions. Furthermore, the strain YJ8 had both *ERG20* and *BTS1* modules, produced 0.7 mg/L miltiradiene.

Because there are additional pathways consuming FPP (Figure 1a), leading to the synthesis of ergosterol, and FOH, the hydrolysis product of FPP, it is expected to obtain a higher miltiradiene production when the efficiency of the conversion of FPP to GGPP is improved. We reasoned that the fusion of BTS1 and ERG20 might enhance the efficiency of this conversion. Thus, we made two modules that produced fusion proteins ERG20-BTS1 and BTS1-ERG20, respectively. While the addition of the *ERG20-BTS1* module (strain YJ9) gave a reduced miltiradiene production as compared to that of the

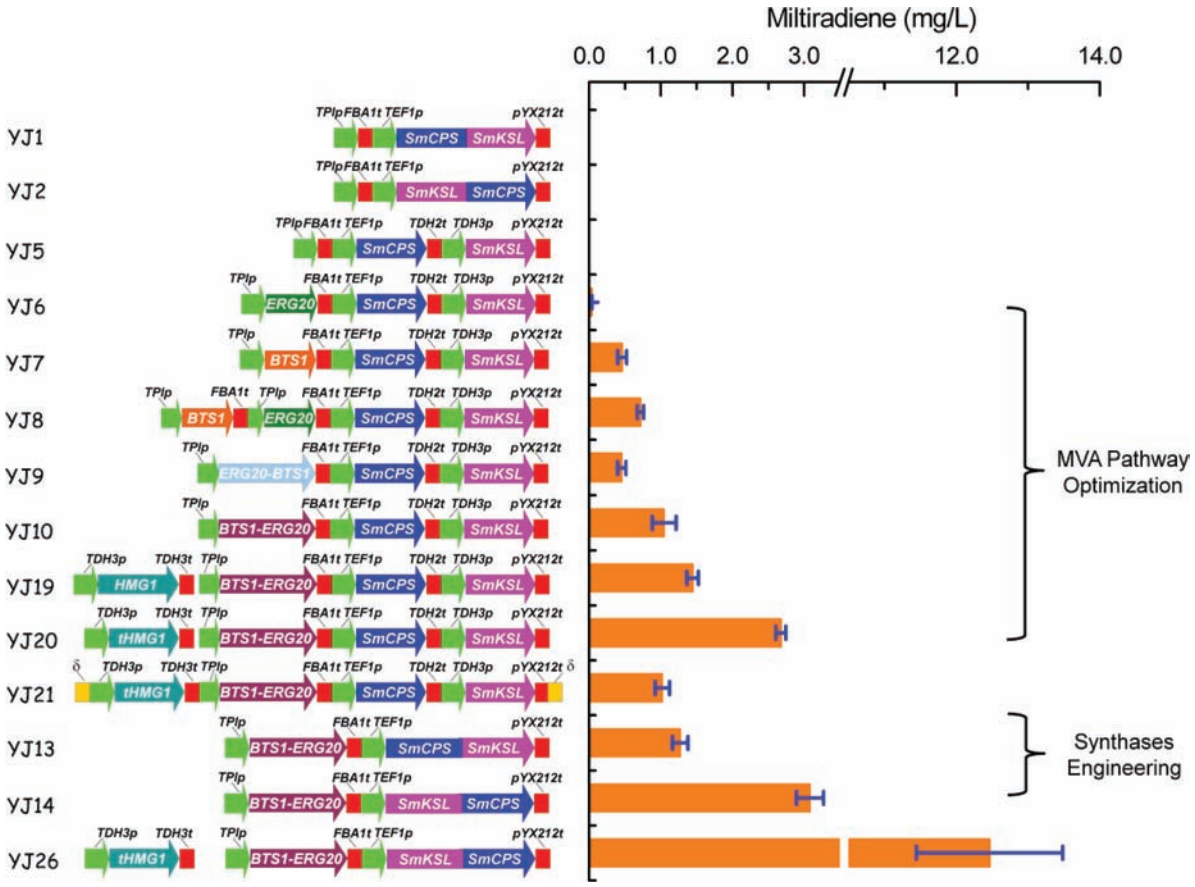

Figure 3. Miltiradiene production by recombinant yeasts harboring modules overproducing various enzymes. The strains were cultivated for 48 h in YPD media, and miltiradiene was extracted with equal volume of *n*-hexane. The data represent the averages ± standard deviations of at least three independent clones.

dx.doi.org/10.1021/ja2114486 | *J. Am. Chem. Soc.* 2012, 134, 3234–3241

strain YJ8, the addition of the *BTS1-ERG20* module (strain YJ10) indeed led to an improved miltiradiene production to 1.0 mg/L. Moreover, the strain YJ10 produced less FOH than other strains including the strain YJ9 (Supporting Information Figure 4). These results indicated the presence of BTS1-ERG20 channeled the FPP flux to miltiradiene production from other FPP-consuming pathways. It should be emphasized that the specific productivity of miltiradiene followed the same trend among these recombinant strains (Supporting Information Figure S3), because these strains had similar growth profiles under shake flask culture conditions.

Another major regulatory control point of the MVA pathway is the formation of MVA from hydroxy-3-methylglutaryl coenzyme A (HMG-CoA) catalyzed by HMG-CoA reductase (HMG) 1 and 2. In *S. cerevisiae*, HMG1 contributes at least 83% of the activity.[15] Early studies showed that the overexpression of the catalytic domain of HMG1 (*tHMG1*) could lead to an improved production of isoprenoids,[16,17] while a recent report showed the full length version was more effective for the production of prenyl alcohols.[18] We thus examined the capacity of both HMG1 and tHMG1 in this study. Additional expression of *HMG1* in the YJ10 background (YJ19) resulted in a 38% increase in miltiradiene yield, and the expression of *tHMG1* (YJ20) led to a 2.6-fold increase to 2.7 mg/L miltiradiene (Figure 3).

As synthetic pathways integrated into chromosome are considered more stable than episomal plasmid-based systems,[19,20] we constructed a strain (YJ21) by integrating the optimized module of YJ20 into the chromosome flanked by two selection markers *URA3* and *HIS3* (Supporting Information Figure S2). However, the integrated strain YJ21 produced only 1.1 mg/L miltiradiene, which was lower than that of the strain YJ20. The lower copy number of the integrated pathway might be the main reason for a reduced miltiradiene production. Although there are more than 300 δ sites on the chromosome of *S. cerevisiae* for integration,[21] it might be difficult to integrate multiple copies of constructs with a recombination of 4 modules in a single transformation experiment. In addition, no selection pressure was applied to enrich strains having multicopy integrations in this study. Developing strategies to further improve integration efficiency should be helpful for the construction of stable strains with higher miltiradiene production capacity. Therefore, all other pathway variants had genes assembled on the plasmid (vide infra).

Miltiradiene Synthases Engineering. We next introduced the BTS1-ERG20 module into the strains with the fused miltiradiene synthases to give the strains YJ13 and YJ14 (Figure 4a). While the combination of BTS1-ERG20 with SmCPS-SmKSL gave a slightly higher miltiradiene production than that of the Strain YJ10, the combination of BTS1-ERG20 with SmKSL-SmCPS gave a 2.9-fold increase to 3.1 mg/L. Further, when *tHMG1* was introduced in the YJ14 background, the resulting strain YJ26 produced 12.5 mg/L miltiradiene, which was a 4.0-fold improvement over the parent strain, carrying separate SmCPS and SmKSL. We also observed that the strain YJ26 produced significantly lower GGOH, the hydrolysis product of GGPP, than the strain YJ20 (Supporting Information Figure S6). These results indicated that the fusion SmKSL-SmCPS was advantageous over the fusion SmCPS-SmKSL as well as the two proteins being expressed separately in terms of transforming GGPP into miltiradiene.

The X-ray crystal structures of two diterpenoids synthases, taxadiene synthase from *Taxus brevifolia* and the class II cyclase

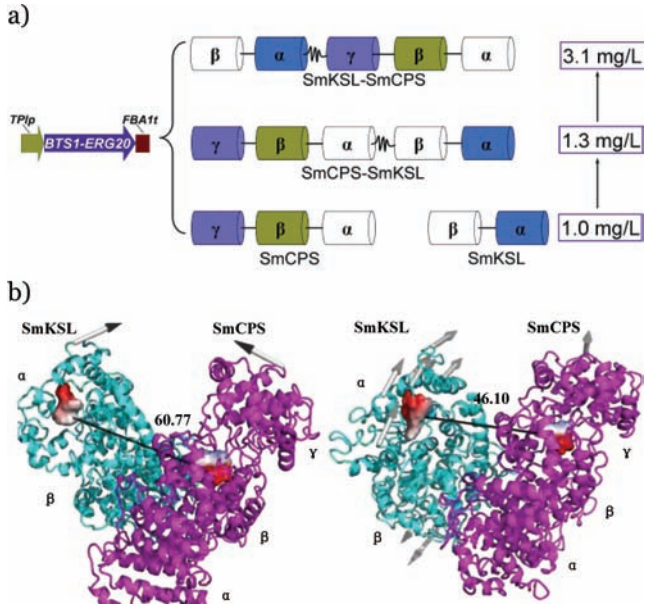

Figure 4. The modeling structures of the fusion enzymes of miltiradiene synthases. (a) The domains arrangement in the primary structure of miltiradiene synthases and their fusions. The white columns indicated the nonfunctional domains, and the colorful columns represented the functional domains. (b) Side view of protein modeling results of SmCPS-SmKSL (left) and SmKSL-SmCPS (right).

ent-copalyl diphosphate synthase from *Arabidopsis thaliana* (AtCPS), have been available recently.[22,23] Protein modeling[24] using AtCPS as the template showed SmCPS belongs to the class II synthase and the active site DXDD motif for H^+-initiated cyclization is located between the $\beta\gamma$ domains in the N-terminus (Supporting Information Figure S7). Protein modeling using taxadiene synthase as the template showed the active site of SmKSL is located at the α domain in the C-terminus (Supporting Information Figure S7). It is conceivable that the fusion protein in the SmKSL-SmCPS format brought the active site of SmCPS and the active α domain of SmCPS closer than that of the SmCPS-SmKSL format (Figure 4a). Indeed, protein modeling showed that active sites in SmKSL-SmCPS have a closer proximity (46.10 Å) than that of SmCPS-SmKSL (60.77 Å). The dynamic behavior derived from normal-mode analysis of these two complexes also showed that the large-scale motion of SmKSL-SmCPS was more favorable for shortening that distance and avoiding the block between two active sites than that of SmCPS-SmKSL (Figure 4b and Supporting Information Figure S7c and d). Therefore, our structural analysis showed protein fusion may bring active sites into a closer proximity, which can be beneficial to miltiradiene production.

Miltiradiene Overproduction by Prototrophic Strains. Because of the *S. cerevisiae* BY4741 background and the presence of pYX212 and p424GPD(HIS) backbone, the above miltiradiene-producing strains remained auxotrophic to leucine and methionine. We further constructed a prototrophic haploid strain YJ28 by complementing the auxotrophic markers *LEU2* and *MET15*. We noticed that *LEU2* and *MET15* complementation improved the cell growth and miltiradiene titer, and that the strain with *LEU2* complementation increased the specific miltiradiene productivity (Figure 5a). The prototrophic strain YJ28 produced 17.9 mg/L miltiradiene in shake flask culture and up to 178 mg/L in 15 L bioreactor culture (Figure 6a),

dx.doi.org/10.1021/ja2114486 | J. Am. Chem. Soc. 2012, 134, 3234−3241

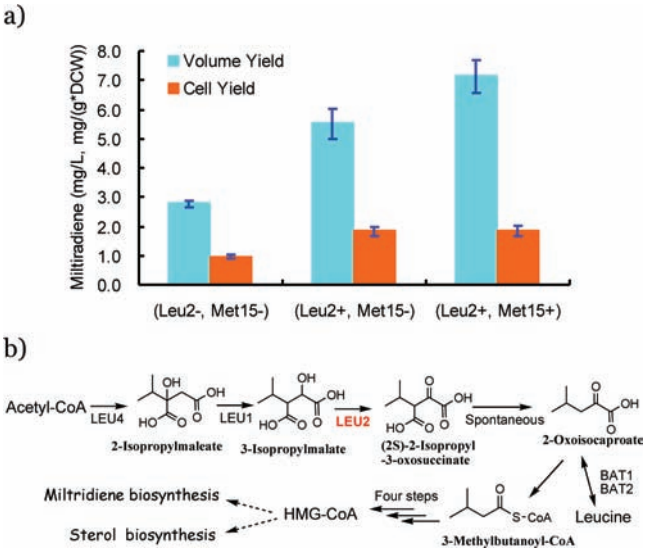

Figure 5. *LEU2* complementation improved miltiradiene productiion. (a) Miltiradiene production by prototrophic and auxotrophic strains in shake flask cultures. (Leu2−, Met15−) represents recombinant strain YJ20 carrying the MVA optimized pathway with methionine and leucine auxotroph, (Leu2+, Met15−) represents recombinant strain YJ25 with methionine auxotroph, and (Leu2+, Met15+) represents prototrophic strain YJ28. Results are the averages ± standard deviations of four independent clones. (b) The proposed alternative HMG-CoA formation pathway involved in leucine metabolism.

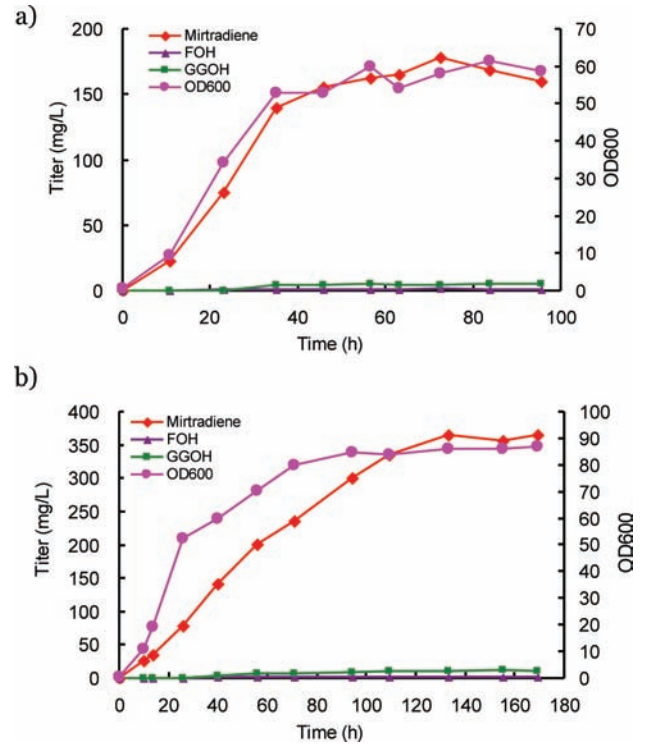

Figure 6. Fermentation profiles of the prototrophic strain YJ28 (a) and the diploid strain YJ2X (b) in a 15 L stirred-tank bioreactor.

which was significantly higher than the previous data of 2.5 mg/L obtained in the recombinant *E. coli* strain.[13] The byproducts FOH and GGOH were only 1.4 and 4.8 mg/L, respectively.

Diploidization is another strategy to improve the productivity due to higher expression levels of heterologous genes and tolerances to various stresses as compared to haploid strains.[19,25] The prototrophic diploid strain YJ2X, constructed by mating the methionine auxotrophic strain YJ27 and BY4742, produced 22.7 mg/L miltiradiene in shake flask culture conditions, which was slightly higher as compared to the haploid strain YJ28. However, when cultivated in a 15 L bioreactor, YJ2X produced 365 mg/L miltiradiene, which was 2.1-fold higher than that of the YJ28 strain. Again, FOH and GGOH were observed at 1.8 and 10.2 mg/L, respectively (Figure 6b). Because the promoters used in our system were all constitutive, no inducers such as IPTG or galactose were required in the culture media. This feature distinguished our study from those previous reports on isoprenoids production in *E. coli* or yeast,[6,7,10,26] and made it more economical and convenient for a large-scale process.

■ DISCUSSION

Early metabolic engineering studies on diterpenoid biosynthesis have been focused on the optimization of the MVA or MEP pathways to increase the precursors supply.[6,11,17] When the cyclization step leading to the core structure of diterpenoids is catalyzed by two consecutive enzymes,[12] no information is available in terms of potential molecular interactions between these enzymes. In the case of miltiradiene production from GGPP catalyzed by SmCPS and SmKSL, we observed interactions between them in vivo with coimmunoprecipitation (Figure 2). Such interaction may be biologically significant, because the formation of protein complex could bring active sites into a closer proximity, facilitating more efficient substrate channeling. In other words, it could prevent intermediates from diffusion and degradation by other enzymes. Indeed, the formation of enzyme complexes has been suggested to improve the efficiency of the specific pathways by preventing substrates and intermediates from diffusion and degradation.[27] Recently, several proteomic studies showed that the formation of protein complexes is common and that the interactions between the consecutive enzymes are helpful for substrate channeling.[28,29] For example, molecular interactions among several enzymes catalyzing the adjacent steps of the tricarboxylic acid cycle in *Bacillus subtilis* were observed for regulating the metabolic fluxes.[30] In human cells, enzymes involved in purine biosynthesis also formed protein complexes.[31] We introduced SmCPS and SmKSL fusions in yeast to improve miltiradiene production, and indeed the fused synthases had better performance. While the pathway variant YJ13 containing the fusion SmCPS-SmKSL only afforded slight improvement as compared to the variant YJ10 with SmCPS and SmKSL being expressed separately, the variant YJ14 contained the reverse fusion SmKSL-SmCPS produced 2.8-fold more miltiradiene (Figure 4). Protein modeling showed that the fusion SmKSL-SmCPS brought the active sites closer than did the fusion SmCPS-SmKSL (Figure 4b). The fact that byproducts GGOH and FOH were less for the variant YJ14 (Supporting Information Figure S6) suggested that GGPP was turned over more efficiently by the fused enzyme SmKSL-SmCPS. As compared to direct evolution of the bifunctional levopimaradiene synthase (LPS) for catalytic activity improvement,[26] engineering the active sites of separate diterpenoid synthases into a close proximity provides another convenient and powerful approach. To test the generality of the approach, we also fused BTS1 and ERG20, enzymes catalyzing the adjacent steps for GGPP production. It turned out that the fusion BTS1-ERG20 was advantageous over the fusion ERG20-BTS1

dx.doi.org/10.1021/ja2114486 | J. Am. Chem. Soc. 2012, 134, 3234−3241

(Supporting Information Figure S4), as the former produced more miltiradiene and less FOH. These results suggested that the fusion BTS1-ERG20 improved the FPP flux to miltiradiene production. The fusion of enzymes within diterpenoid biosynthetic pathway avoided the loss of intermediates through diffusion, degradation, or conversion by competitive enzymes in multistep metabolic pathways,[32] which was similar to the natural megasynthases systems such as Type I polyketide synthase and fatty acid synthase.[33]

It is worth mentioning that the introduction of SmCPS and SmKSL or their fusions into the yeast resulted in no miltiradiene production (Figure 3). These observations may otherwise lead to conclusions that those enzymes were incompetent in yeast, or that those genes were incorrectly expressed. Thanks to the MOPE strategy, we were able to assemble pathway variants by including genes responsible for the formation of metabolites beyond miltiradiene per se. Although the MOPE strategy is technically reminiscent of "DNA assembler" described earlier,[14] the efficiency for the construction of functional modules was substantially improved with one-step SOE PCR. Because all promoter and terminator sequences were purposely included at the termini of each module, the assembled pathway variants essentially had no redundant DNA sequences. Moreover, the MOPE strategy did not limit modules to heterologous genes, as chimeric pathways containing heterologous and endogenous genes were efficiently assembled in this study. Thus, we noticed the overexpression of *ERG20* in the YJ5 background resulted in little improvement in miltiradiene production, which was similar to a number of previous reports on isoprenoids production.[7,34,35] However, the expression of *BTS1* resulted in significantly higher miltiradiene production, indicating that GGPP synthesis was the pivotal step to provide extra metabolic flux for miltiradiene production. Similar observations have been documented for the production of other diterpenoids.[35−37] Early studies showed that the higher level of HMG reductase (HMG1) as well as its catalytic domain tHMG1 were helpful for the isoprenoid biosynthesis.[16−18] We found that overexpression of both *HMG1* and *tHMG1* in the YJ10 background led to an improved miltiradiene production yield (Figure 3a). However, overexpression of eithor HMG1 (YJ16) or tHMG1 (YJ17) in the YJ5 background produced little miltiradiene (Supporting Information Figure 5). These results indicated in our system that BTS1, but not HMG1, played the most important role in directing the metabolic flux to miltiradiene biosynthesis.

We further constructed the prototrophic haploid strain YJ28 and diploid strain YJ2X, and achieved major improvement in terms of miltiradiene titer at a large-scale culture. The prototrophic haploid strains grew faster and produced more miltiradiene than those auxotrophic strains. Interestingly, the *LEU2* complementation improved the specific miltiradiene productivity, while the *MET15* complementation had no such effect, indicating that leucine supply was beneficial for miltiradiene biosynthesis. It occurred to us that leucine metabolism may be networked with isoprenoid biosynthesis (Figure 5b). A previous report showed that leucine catabolism could lead to the formation of HMG-CoA and the incorporation into sterol in *Leishmania mexicana*.[38] The biosynthesis of leucine produces a precursor 2-oxoisocaproate, and exogenous leucine can be catabolized to this precursor. 2-Oxoisocaproate can be converted into HMG-CoA by a number of enzymes. Therefore, the leucine biosynthetic pathway may be considered as a bypath to facilitate additional HMG-CoA supply. Our observation cautioned one to consider metabolisms beyond the biosynthetic genes and to use leucine prototrophic hosts for a higher isoprenoids production.

In summary, we demonstrated remarkable improvement of miltiradiene productivity by using the MOPE strategy in the construction of flexible pathway variants involving multiple genes in *S. cerevisiae*. Furthermore, protein fusion was shown to be general in directing metabolic flux to focused pathway for the heterologous production of isoprenoids such as miltiradiene. Strategies of pathway assembling in this study should be applicable to engineering microbial hosts for the production of other valuable metabolites.

EXPERIMENTAL PROCEDURES

Strains, Reagents, and Media. The yeast strains used in this study are listed in Supporting Information Table 1. PrimeStar DNA polymerase, restriction enzymes, and other enzymes were purchased from TaKaRa Bio. Oligonucleotides were purchased from Invitrogen. DNA gel purification and plasmid extraction kits were purchased from Beyotime. Yeast nitrogen base and peptone were products of Difco. Yeast extracts and tryptone were from Oxoid. Amino acids, nucleotides, and agar powder were supplied by Dingguo Biotech. Anti-Flag M2 affinity agarose, mouse Flag antibodies, prenyl alcohols (FOH, GGOH), and other chemicals were purchased from Sigma. Mouse c-Myc antibodies were from Santa Cruz. Enhanced chemoluminescence and PVDF membrane were from Amersham Biosciences. Synthetic dextrose (SD) medium consisted of 20 g/L glucose, 6.7 g/L yeast nitrogen base with $(NH_4)_2SO_4$ and without amino acids. SD containing one or several specific nutrients (20 mg/L uracil, 20 mg/L histidine, 20 mg/L methionine, or 100 mg/L leucine) was used for the corresponding auxotrophic strains cultivation. YPD consisted of 10 g/L yeast extract, 20 g/L peptone, and 20 g/L dextrose. *Escherichia coli* strains were grown at 37 °C on Luria−Bertani medium (10 g/L tryptone, 5 g/L yeast extract, 10 g/L NaCl) supplemented with ampicillin (100 ug/mL) if required. Agar plates were made with the corresponding liquid medium supplemented with 15 g/L agar powder. The medium for a large-scale culture using 15 L stirred-tank bioreactor was comprised of 20 g/L glucose, 10 g/L yeast extract, 20 g/L peptone, 10 g/L $(NH_4)_2SO_4$, 1.0 g/L KH_2PO_4, 1.0 g/L $MgSO_4{\cdot}7H_2O$, and 1.0 g/L $CaCl_2{\cdot}2H_2O$.

DNA Manipulation. All of the primers used for DNA manipulation were listed in Supporting Information Table 2. The gene expressing modules consisted of a promoter, a structural gene, a terminator, and the promoter of the next module for homologous recombination. The promoter *TPIp* and the terminator *pYX212t* were PCR-amplified from pYX212, which also was used as an expression vector kindly provided by Prof. Ming Yan at Nanjing University of Technology; other prompters (*TEF1p* and TDH3p), terminators (*FBA1t*, *CYC1t* and *ADH2t*), and functional genes (*BTS1*, *ERG20* and *HMG1*) were PCR-amplified from the genomic DNA of *S. cerevisiae* BY4741. *SmCPS* and *SmKSL* were PCR-amplified from the cDNA cloning vectors.[13] The fusion enzymes encoding genes were constructed by inserting a widely used GGGS linker encoding sequence "GGT GGT GGT TCT" between the two corresponding genes.[36,39] All modules were constructed with the one-step PCR strategy similar to overlap extension PCR. Briefly, purified parts of individual module (promoter, functional gene, terminator, and promoter of next module, molar ratio 1:3:3:1) were mixed in about 100−300 ng each, then were added 3 μL of dNTP (2.5 mM each), 5 ul 5 × PrimerStar buffer, 1.25 U PrimeSTAR HS DNA polymerase, and H_2O to a total volume of 25 μL, and then it was subjected to PCR amplification with the thermocycle conditions of 95 °C for 5 min, 15 cycles of 98 °C for 10 s, 68 °C for 1 min/kb, and last 68 °C for 10 min. Next, 2 μL of unpurified PCR products was taken out as the template and added F- and R-primer and PrimeSTAR HS DNA polymerase and for normal PCR amplification in a total volume of 100 μL according to manufacturer's instructions. The DNA fragments of parts and modules were individually gel-purified from a 0.8% agarose gel. Equal molar

dx.doi.org/10.1021/ja2114486 | J. Am. Chem. Soc. 2012, 134, 3234−3241

amounts of purified individual modules (300−500 ng) were mixed and transformed into *S. cerevisiae* with electroporation at 1.5 kV, 10 μF, and 200 Ω in a 0.2 cm gap electroporation cuvette using Eppendorf Eporator (Eppendorf AG, Hamburg, Germany). p424GPD(HIS) used for overexpressing *HMG1* or *tHMG1* was constructed by replacing *TRP1* marker with *HIS3* in p424GPD[40] using RF cloning method as previous described.[41] Next, the *HMG1* or *tHMG1* was cloned to the downstream of the *TDH3p* promoter using RF cloning strategy as mentioned above. The leucine and/or methionine auxotrophic strains were constructed as a previous report.[19] Diploid strain YJ2X was constructed by mating the methionine auxotrophic strain YJ27 and BY4742 as described previously.[25]

Verification of the Assembled Pathways. Selected colonies formed on the plates were cultured in 5 mL of YPD liquid medium at 30 °C for 72 h. Cells were collected and disrupted using ethanol-washed glass beads (0.4 g, 0.4−0.6 mm). Cell lysates were collected for plasmid extraction using plasmid extraction kit according to manufacturer's instructions. Recovered plasmids were checked by designed PCR procedures to verify the assembled pathways. Alternatively, positive plasmids were also transformed into *E. coli* DH5α, recovered, digested by the restriction endonuclease Hind III, and analyzed by gel electrophoresis.

Extraction and Quantification of Isoprenoids. Miltiradiene samples were purified in house. Briefly, cell pellets of the engineered *S. cerevisiae* were extracted with hexane three times. The hexane phase was pooled and evaporated in vacuum, and the residues were subjected to column chromatography on silica gel eluted with hexane to give miltiradiene with good purity. GC−MS and NMR data of a purified sample were shown (Supporting Information Figures 8−10).

To quantify yields of miltiradiene and prenyl alcohols (FOH, GGOH) of different cultures, 100 mL of hexane was mixed with 100 mL of culture broth (including yeast cells) and vortexed for 30 min. The organic layer was recovered, and concentrated to a final volume of 0.5 mL. The concentrated samples were subjected to GC analysis. The isoprenoids were quantified on the 7890F GC instrument (Techcomp Scientific Instrument Co. Ltd., Shanghai, China) equipped with a flame ionization detector. GC analysis was done with a SE-54 column (30 m × 0.25 mm × 0.25 μm), and operational conditions were as follows. The carrier gas nitrogen was set at a flow rate of 1.6 mL/min. The oven temperature was first kept constant at 40 °C for 10 min, and then increased to 200 °C at the increment of 10 °C/min, and held for 40 min at the final temperature. Temperatures for the injector and the detector were at 250 and 280 °C, respectively.

Cultivation Procedures for Miltiradiene Production. To determine the performance of recombinant yeast strains, individual clones were transferred into the SC medium lacking the corresponding nutrition and cultivated at 30 °C, 200 rpm for 48 h. Aliquots were diluted to an initial OD_{600} of 0.05 in 100 mL of YPD medium in 500 mL flasks and grown at 30 °C, 200 rpm for 48 h. The culture samples were analyzed as described above.

For a larger-scale culture with the 15 L stirred-tank bioreactor (Shanghai Guoqiang Bioengineering Equipment Co. Ltd., Shanghai, China), 6 L of fermentation medium was inoculated at 10 vol % with the preculture of the recombinant yeast prepared in a shake flask at 30 °C, 200 rpm for 48 h. The dissolved oxygen, temperature, aeration, and pH were controlled at >40% saturation, 30 °C, 1 volume of air per volume of culture per minute and 5.5, respectively. Concentrated glucose solution (100%, wt/vol) was fed periodically to keep the glucose concentration above 1.0 g/L. Dodecane was added to 20% (v/v) of the media volume. Additional yeast extract (10 g/L) and peptone (20 g/L) were fed at 35.2 h for YJ28 growth, and $(NH_4)_2SO_4$ solution (10 g/L) was fed at 39.9 h for YJ2X fermentation. Duplicate culture aliquots were collected periodically to determine glucose concentration, cell density, and miltiradiene content.

Immunoprecipitation Analysis. Transfection cells were cultivated for 48 h, and washed four times with ice-cold PBS buffer. The cells were disrupted at 4 °C with sonication (200 W, 2 s sonication and 1 s rest, 30 times) in 1 mL of cell lysis buffer (20 mM HEPES, PH 7.2, 50 mM NaCl, 0.5% TritonX-100, 1 mM NaF, and 1 mM DTT plus protease inhibitors). The lysates were centrifuged for 10 min at 12 000*g* at 4 °C, and the supernatants were combined with 20 μL of anti-Flag M2 affinity agarose (Sigma) and mixed for 8 h at 4 °C. The immunoadsorbents were recovered by centrifugation for 5 min at 1000*g* in cell lysis buffer and washed two times with NETN buffer (20 mM Tris, 100 mM NaCl, 0.5% NP-40, and 1 mM EDTA plus protease and phosphatase inhibitors, pH 7.5). Next, 50 μL of loading buffer was added to the immunoabsorbents and boiled for 10 min. The eluted samples were subjected to SDS-PAGE and immune-blot analysis as described previously.[42]

Protein Modeling. Detailed computational protein structure modeling methods for SmCPS-SmKSL and SmKSL-SmCPS were described in the figure legend of Supporting Information Figure 7.

■ ASSOCIATED CONTENT

Ⓢ Supporting Information

Table S1: *S. cerevisiae* strains used in this study. Table S2: Primers used for part cloning and module construction. Figure S1: Hypothetical tanshinones biosynthetic pathway. Figure S2: Schematic illustration of the modular pathway engineering strategy for rapid pathway construction. Figure S3: The specific miltiradiene titer in recombinant *S. cerevisiae* strains. Figure S4: BTS1-ERG20 fusion decreased FOH level. Figure S5: The BTS1 not the tHMG1 was the key enzyme for miltiradiene production. Figure S6: SmKSL-SmCPS fusion decreased FOH and GGOH levels. Figure S7: The modeling structures of SmCPS and SmKSL. Figure S8: GC−MS of purified miltiradiene from the engineered yeast strain. Figure S9: ^{13}C NMR spectra of miltiradiene. Figure S10: ^{1}H NMR spectra of miltiradiene. This material is available free of charge via the Internet at http://pubs.acs.org.

■ AUTHOR INFORMATION

Corresponding Author

zhaozb@dicp.ac.cn; huangluqi@263.net

Author Contributions

[▽]These authors contributed equally.

Notes

The authors declare no competing financial interest.

■ ACKNOWLEDGMENTS

This work was supported by the National Natural Science Foundation of China (no. 81072990 and no. 30901965). We also thank Prof. Shengli Yang of Shanghai Institute for Biological Sciences, CAS, for his suggestions.

■ REFERENCES

(1) Hanson, J. R. *Nat. Prod. Rep.* **2007**, *24*, 1332−1341.
(2) Rowinsky, E. K. *Annu. Rev. Med.* **1997**, *48*, 353−374.
(3) Wang, B. Q. *J. Med. Plants Res.* **2010**, *4*, 2813−2820.
(4) Chang, M. C.; Keasling, J. D. *Nat. Chem. Biol.* **2006**, *2*, 674−681.
(5) Keasling, J. D. *Science* **2010**, *330*, 1355−1358.
(6) Ajikumar, P. K.; Xiao, W.-H.; Tyo, K. E. J.; Wang, Y.; Simeon, F.; Leonard, E.; Mucha, O.; Phon, T. H.; Pfeifer, B.; Stephanopoulos, G. *Science* **2010**, *330*, 70−74.
(7) Ro, D.-K.; Paradise, E. M.; Ouellet, M.; Fisher, K. J.; Newman, K. L.; Ndungu, J. M.; Ho, K. A.; Eachus, R. A.; Ham, T. S.; Kirby, J.; Chang, M. C. Y.; Withers, S. T.; Shiba, Y.; Sarpong, R.; Keasling, J. D. *Nature* **2006**, *440*, 940−943.
(8) Na, D.; Kim, T. Y.; Lee, S. Y. *Curr. Opin. Microbiol.* **2010**, *13*, 363−370.
(9) Redding-Johanson, A. M.; Batth, T. S.; Chan, R.; Krupa, R.; Szmidt, H. L.; Adams, P. D.; Keasling, J. D.; Lee, T. S.; Mukhopadhyay, A.; Petzold, C. J. *Metab. Eng.* **2011**, *13*, 194−203.

(10) Dueber, J. E.; Wu, G. C.; Malmirchegini, G. R.; Moon, T. S.; Petzold, C. J.; Ullal, A. V.; Prather, K. L. J.; Keasling, J. D. *Nat. Biotechnol.* **2009**, *27*, 753−759.
(11) Morrone, D.; Lowry, L.; Determan, M. K.; Hershey, D. M.; Xu, M. M.; Peters, R. J. *Appl. Microbiol. Biotechnol.* **2010**, *85*, 1893−1906.
(12) Cao, R.; Zhang, Y. H.; Mann, F. M.; Huang, C. C.; Mukkamala, D.; Hudock, M. P.; Mead, M. E.; Prisic, S.; Wang, K.; Lin, F.-Y.; Chang, T.-K.; Peters, R. J.; Oldfield, E. *Proteins* **2010**, *78*, 2417−2432.
(13) Gao, W.; Hillwig, M. L.; Huang, L. Q.; Cui, G. H.; Wang, X. Y.; Kong, J. Q.; Yang, B.; Peters, R. J. *Org. Lett.* **2009**, *11*, 5170−5173.
(14) Shao, Z.; Zhao, H. M. *Nucleic Acids Res.* **2009**, *37*, e16.
(15) Basson, M. E.; Thorsness, M.; Rine, J. *Proc. Natl. Acad. Sci. U.S.A.* **1986**, *83*, 5563−5567.
(16) Donald, K. A.; Hampton, R. Y.; Fritz, I. B. *Appl. Environ. Microbiol.* **1997**, *63*, 3341−3344.
(17) Engels, B.; Dahm, P.; Jennewein, S. *Metab. Eng.* **2008**, *10*, 201−206.
(18) Ohto, C.; Muramatsu, M.; Obata, S.; Sakuradani, E.; Shimizu, S. *Appl. Microbiol. Biotechnol.* **2009**, *82*, 837−845.
(19) Tokuhiro, K.; Muramatsu, M.; Ohto, C.; Kawaguchi, T.; Obata, S.; Muramoto, N.; Hirai, M.; Takahashi, H.; Kondo, A.; Sakuradani, E.; Shimizu, S. *Appl. Environ. Microbiol.* **2009**, *75*, 5536−5543.
(20) Tyo, K. E.; Ajikumar, P. K.; Stephanopoulos, G. *Nat. Biotechnol.* **2009**, *27*, 760−765.
(21) Dujon, B. *Trends Genet.* **1996**, *12*, 263−270.
(22) Koksal, M.; Jin, Y.; Coates, R. M.; Croteau, R.; Christianson, D. W. *Nature* **2011**, *469*, 116−120.
(23) Koksal, M.; Hu, H.; Coates, R. M.; Peters, R. J.; Christianson, D. W. *Nat. Chem. Biol.* **2011**, *7*, 431−433.
(24) Bordoli, L.; Kiefer, F.; Arnold, K.; Benkert, P.; Battey, J.; Schwede, T. *Nat. Protoc.* **2009**, *4*, 1−13.
(25) Yamada, R.; Taniguchi, N.; Tanaka, T.; Ogino, C.; Fukuda, H.; Kondo, A. *Biotechnol. Biofuels* **2011**, *4*, 8.
(26) Leonard, E.; Ajikumar, P. K.; Thayer, K.; Xiao, W.-H.; Mo, J. D.; Tidor, B.; Stephanopoulos, G.; Prather, K. L. J. *Proc. Natl. Acad. Sci. U.S.A.* **2010**, *107*, 13654−13659.
(27) Srere, P. A. *Annu. Rev. Biochem.* **1987**, *56*, 89−124.
(28) Menon, A. L.; Poole, F. L. II; Cvetkovic, A.; Trauger, S. A.; Scott, J. W.; Shanmukh, S.; Praissman, J.; Jenney, F. E. Jr.; Wikoff, W. R.; Apon, J. V.; Siuzdak, G.; Adams, M. W. W. *Mol. Cell. Proteomics* **2009**, *8*, 735−751.
(29) Kühner, S.; van Noort, V.; Betts, M. J.; Leo-Macias, A.; Batisse, C.; Rode, M.; Yamada, T.; Maier, T.; Bader, S.; Beltran-Alvarez, P.; Castaño-Diez, D.; Chen, W.-H.; Devos, D.; Güell, M.; Norambuena, T.; Racke, I.; Rybin, V.; Schmidt, A.; Yus, V.; Aebersold, R.; Herrmann, R.; Böttcher, B.; Frangakis, A. S.; Russell, R. B.; Serrano, L.; Bork, P.; Gavin, A.-C. *Science* **2009**, *326*, 1235−1240.
(30) Meyer, F. M.; Gerwig, J.; Hammer, E.; Herzberg, C.; Commichau, F. M.; Völker, U.; Stülke, J. *Metab. Eng.* **2011**, *13*, 18−27.
(31) An, S.; Kumar, R.; Sheets, E. D.; Benkovic, S. J. *Science* **2008**, *320*, 103−136.
(32) Conrado, R. J.; Varner, J. D.; DeLisa, M. P. *Curr. Opin. Biotechnol.* **2008**, *19*, 492−499.
(33) Smith, S.; Tsai, S. C. *Nat. Prod. Rep.* **2007**, *24*, 1041−1072.
(34) Jackson, B. E.; Hart-Wells, E. A.; Matsuda, S. P. *Org. Lett.* **2003**, *5*, 1629−1632.
(35) Ohto, C.; Muramatsu, M.; Obata, S.; Sakuradani, E.; Shimizu, S. *Appl. Microbiol. Biotechnol.* **2010**, *87*, 1327−1334.
(36) Ukibe, K.; Hashida, K.; Yoshida, N.; Takagi, H. *Appl. Environ. Microbiol.* **2009**, *75*, 7205−7211.
(37) Kai, G. Y.; Xu, H.; Zhou, C. C.; Liao, P.; Xiao, J. B.; Luo, X. Q.; You, L. J.; Zhang, L. *Metab. Eng.* **2011**, *13*, 319−327.
(38) Ginger, M. L.; Chance, M. L.; Sadler, I. H.; Goad, L. J. *J. Biol. Chem.* **2001**, *276*, 11674−11682.
(39) Aslan, F. M.; Yu, Y.; Mohr, S. C.; Cantor, C. R. *Proc. Natl. Acad. Sci. U.S.A.* **2005**, *102*, 8507−8512.
(40) Mumberg, D.; Muller, R.; Funk, M. *Gene* **1995**, *156*, 119−122.
(41) Zhou, Y. J.; Yang, F.; Zhang, S. F.; Tan, H. D.; Zhao, Z. K. *World J. Microbiol. Biotechnol.* **2011**, *27*, 2999−3003.
(42) Salim, K.; Fenton, T.; Bacha, J.; Urien-Rodriguez, H.; Bonnert, T.; Skynner, H. A.; Watts, E.; Kerby, J.; Heald, A.; Beer, M.; McAllister, G.; Guest, P. G. *J. Biol. Chem.* **2002**, *277*, 15482−15485.